

Expression and characterization of the flavoprotein domain of gp91^{phox}

Chang-Hoon Han and Mun-Han Lee¹

Department of Biochemistry, Swiss Federal Institute of Technology in Zurich, Universitatstrasse 16, 8092 Zurich, Switzerland

¹Department of Biochemistry, College of Veterinary Medicine, Seoul National University, Suwon 441-744, Korea

Truncated forms of gp91^{phox} were expressed in *E. coli* in which the N-terminal hydrophobic transmembrane region was replaced with a portion of the highly soluble bacterial protein thioredoxin (TRX). TRX-gp91^{phox} (306-569), which contains the putative FAD and NADPH binding sites, showed NADPH-dependent NBT (nitroblue tetrazolium) reductase activity, whereas TRX-gp91^{phox} (304-423) and TRX-gp91^{phox} (424-569) were inactive. Activity saturated at about a 1:1 molar ratio of FAD to TRX-gp91^{phox} (306-569), and showed the same Km for NADPH as that for superoxide generating activity by the intact enzyme. Activity was not inhibited by superoxide dismutase, indicating that it was not mediated by superoxide, but was blocked by an inhibitor of the respiratory burst oxidase, diphenylene iodonium (DPI). In the presence of Rac1, the cytosolic regulatory protein p67^{phox} stimulated the NBT reductase activity, but p47^{phox} had no effect. Truncated p67^{phox} containing the activation domain (residues 199-210) stimulated activity approximately 2-fold, whereas forms mutated or lacking this region failed to stimulate the activity. Our data indicate that: 1) TRX-gp91^{phox} (306-569) contains the binding sites for both pyridine and flavin nucleotides; 2) this flavoprotein domain shows NBT reductase activity; and 3) the flavin-binding domain of gp91^{phox} is the target of regulation by the activation domain of p67^{phox}.

Key words: gp91^{phox}, FAD and NADPH binding sites; NBT reductase activity.

Introduction

Neutrophils and macrophages produce superoxide (O₂⁻) and secondary reactive oxygen species (H₂O₂, HOCl) that participate in killing of phagocytized microorganisms [1, 7, 44, 5]. Superoxide generation is catalyzed by a multicomponent enzyme, the respiratory burst oxidase or

NADPH oxidase. The catalytic moiety is a plasma membrane associated flavocytochrome b₅₅₈ which is composed of two subunits gp91^{phox} and p22^{phox} [29, 35, 45, 40, 21]. The flavocytochrome is inactive in resting cells, but upon cell stimulation, the flavocytochrome is activated by assembly with the cytosolic regulatory proteins p47^{phox} [6, 11, 19, 50] and Rac (Rac2 and/or Rac1) [36, 20, 13].

The large subunit of the flavocytochrome, gp91^{phox} has a highly hydrophobic N-terminus which is predicted to contain 5~6 transmembrane helices [41, 12, 49]. The flavocytochrome contains two hemes [31, 8], which reside solely in gp91^{phox} [54] as well as a single FAD [31, 23, 14]. Various models [8, 54] suggest that the heme groups both reside within the hydrophobic N-terminal half of the molecule, and specific histidines within this region have been suggested as heme ligands. The relatively hydrophilic C-terminal half of gp91^{phox} is homologous to several flavoprotein dehydrogenases, particularly in putative FAD and NADPH binding sequences [39, 43, 47] (Fig. 1), and is therefore predicted to form an independently folding flavoprotein domain. Direct binding of native FAD and FAD analogs to flavocytochrome b₅₅₈ has been demonstrated by several groups [31, 14, 39]. Localization of the FAD binding region is predicted from studies using plasma membranes from a chronic granulomatous disease patient with a point mutation at His-338, which showed low FAD content in plasma membrane and failed to produce superoxide [53]. The location of the NADPH binding site is not well established. Although gp91^{phox} contains regions homologous to known NADPH binding sites (Fig. 1), direct binding of NADPH or NADP⁺ has not been demonstrated. Different affinity labeling analogs of NADPH show binding to either gp91^{phox} [38, 15] or p67^{phox} [46]. The latter result has led to the suggestion that p67^{phox} contains the binding site for pyridine nucleotide (or a portion thereof) and that activation might involve bringing this binding site into juxtaposition with the flavin moiety on the flavocytochrome [46].

Individual role for the cytosolic regulatory proteins in activating the NADPH oxidase have been proposed in recent studies. p47^{phox} functions as a regulated adapter

*Corresponding author

Phone: 82-31-290-2741; Fax: 82-31-293-0084

E-mail: vetlee@snu.ac.kr

protein in a cell-free system; while it is not essential for cell-free NADPH oxidase activity, it increases the affinity of p67^{phox} and Rac1 by about 2 orders of magnitude [16, 24]. Both Rac and p47^{phox} provide binding sites for p67^{phox}, and Rac may function similarly to p47^{phox} in binding and anchoring p67^{phox} (i.e., both may be regulated adapter proteins). We have proposed that it is p67^{phox} that is the direct regulator of electron transfers within the flavocytochrome. An “activation domain” localized within amino acid residues 199~210 in p67^{phox} is essential for cell-free NADPH oxidase activity [18], and a point mutation at residue 204 eliminates NADPH oxidase activity without affecting either the binding of p67^{phox} to p47^{phox} or Rac, or the assembly of the mutant p67^{phox} in the NADPH oxidase complex [18]. The target for this activation domain on p67^{phox} is unknown, but we hypothesize that it is localized within the flavoprotein domain of gp91^{phox}.

In this study, we have investigated the putative flavoprotein domain of gp91^{phox}. The hydrophobic transmembrane heme-containing domain was eliminated and replaced by a highly soluble portion of bacterial thioredoxin. Using TRX-gp91^{phox} (306~569), which is predicted to contain both FAD and NADPH binding sites, the NADPH diaphorase activity was detected and investigated. Our results indicate that this domain contains both the NADPH and FAD binding sites. In addition, the flavoprotein domain responds to regulation by p67^{phox} and Rac, indicating the presence of interaction regions for one or both of these factors.

Materials and Methods

Truncation of gp91^{phox}:

Truncated gp91^{phox} clones were obtained by PCR using gp91^{phox} DNA cloned in the pGEX-2T plasmid as the template. The forward primers (CGTGGATCCCCTTTC AAAACCATCGACCTA for 304~423, CGTGGATCCGGT ACAAATATTGCAATAAC for 424~569, and CGTGGATCC AAAACCATCGAGCTACAGATG for 306~569) were designed to introduce a BamHI site (shown in boldface). The reverse primers (CGTAAGCTTTTAGACTGACTTG AGAATGGATGC for 304~423, CGTAAGCTTTTAGAAG TTTTCCTTGTTGAAAAT for both 306~569 and 424~569) were designed to introduce a Hind III site (shown in boldface) and a stop codon (underlined). These PCR products were purified with a PCR purification kit (Qiagen), and were digested with BamHI and Hind III. The digested samples were purified by 1% agarose gel electrophoresis, and extracted from agar by gel extraction kit (Qiagen). The purified DNA fragments were ligated into the BamHI and Hind III sites of pET-32a(+) vector, and then transformed into BL21 (DE3). Transformants were selected from LB/ampicillin plates, and plasmids were isolated from 2 ml cultures of transformants as

described previously [42]. The plasmids were digested with BamH I and Hind III, and were separated on 1% agarose to confirm the presence of the insert. The clones were sequenced to rule out unexpected mutations and to confirm the truncations.

Expression and purification of recombinant proteins:

Recombinant proteins p47^{phox} and wild-type p67^{phox} were expressed in insect cells (sf9 cell) and purified according to Ulinger et al. [51,52]. Rac1 cDNA cloned in pGEX-2T was expressed in DH5a cells as a GST fusion form, and purified by binding to glutathione-Sepharose followed by thrombin cleavage [26]. Truncated and point mutated forms of p67^{phox}-GST fusions were expressed and purified as above except that thrombin was not used and proteins were eluted with 100 mM glutathione [18].

For preparation of TRX-tgp91^{phox} fusion proteins, *E. coli* were grown at 37°C in LB media (1 L) to an A₅₅₀ of 0.4. IPTG (1 mM) was added and cells were shaken at 37°C for 4 hrs. Except for the 424~569 form, truncated forms of gp91^{phox} were initially insoluble. These were solubilized and renatured according to a modification of the method of Gentz et al. [17]. Cells were pelleted by centrifuging at 4,500 × g for 15 min, were resuspended in 6 M guanidine HCl, pH 7.8, 50 mM Tris-HCl, 500 mM NaCl and incubated on ice for 1 hr. Insoluble material was removed by centrifugation at 30,000 × g × 20 min. The supernatant was applied to a nickel chelate affinity resin (ProBond, Invitrogen), which was washed 3 times with several volumes of wash buffer (8 M urea, 500 mM NaCl, 50 mM Tris-HCl, pH 7.8). The protein was eluted with the same buffer containing 500 mM imidazole. Dithiothreitol (DTT) (2 mM) was added and samples were sequentially dialyzed for 5 hrs each against a series of buffers containing 2 mM DTT plus 1 M urea, 0.2 M urea, and then no urea. DTT was removed after the final step by dialysis against 500 mM NaCl, 50 mM Tris-HCl, pH 7.8. Protein concentration was determined according to Bradford [4] and samples were stored at –80°C before use.

NBT reductase activity assay:

NBT reductase activity was determined using a Thermomax Kinetic Microplate reader (Molecular Devices, Menlo Park, CA). Expressed forms of gp91^{phox} were preincubated in most experiments with an equimolar ratio of FAD (or, in the case of the FAD titration, with varying ratios of FAD/protein) for 16 hrs at 4°C before use. The incubation contained 4 μM of FAD-preloaded TRX-gp91^{phox} (306~569), 200 mM arachidonate, combinations of cytosolic regulatory proteins [4.8 mM p67^{phox}, 4.2 mM p47^{phox}, and/or 5.4 mM Rac1 which had been preloaded with GTPγS (4)], all in a 50 ml volume of assay buffer (100 mM KCl, 3 mM NaCl, 4 mM MgCl₂, 1 mM EGTA, and 10 mM PIPES, pH 7.0). DPI was prepared as a 1 mM stock solution in DMSO, and

working solutions were prepared by dilution into assay buffer. An extinction coefficient of 15.1 mM⁻¹ cm⁻¹ at 264 nm was used to determine its concentration [37]. Three 10 ml aliquots of each reaction mixture were transferred to 96-well assay plates and preincubated for 5 min at 25°C. 240 µl of assay buffer containing 200 mM NADPH and 200 mM NBT was added to each well. NBT reduction was quantified by monitoring absorbance change at 595 nm using an extinction coefficient of 12.6 mM⁻¹ cm⁻¹ at 595 nm [28].

Results

Expression of TRX-fusion forms of truncated gp91^{phox}:

The expression strategy was designed based on the idea that the C-terminal half of gp91^{phox} is relatively hydrophilic, and that this domain will fold independently. We initially constructed a series of truncated mutant as the N-terminal GST fusion proteins and His₆ fusions. Those were; gp91^{phox} (190~569), (228~569), (304~569), (424~569), and (304~423). All constructs except for gp91^{phox} (190~569), which contains a large hydrophobic segment, were expressed at high levels in *E. coli*. However, neither GST nor His₆ fusion forms were soluble, and denaturation/renaturation methods (vide infra) failed to generate soluble products.

In contrast, the thioredoxin fused forms of truncated gp91^{phox} [TRX-gp91^{phox} (304~569), TRX-gp91^{phox} (424~569), and TRX-gp91^{phox} (306~569)] were successfully expressed and were readily solubilized using a urea unfolding/refolding method (Fig. 2). TRX-gp91^{phox} (228~569) was also expressed, but it was not possible to solubilize this form. The largest form of the soluble protein, TRX-gp91^{phox} (306~569) is predicted based on sequence homology to contain binding sites for both FAD and NADPH (Fig. 1). The highly soluble TRX domain reportedly improves the solubility of proteins to which it is fused [27], and the vector also encodes a hexa histidine which allows purification under denaturing condition on a

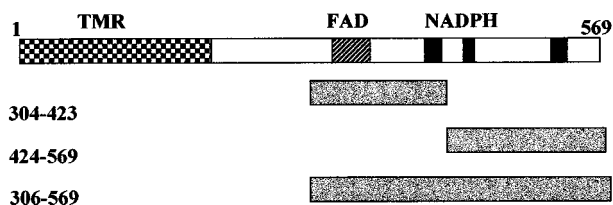


Fig 1. Truncations of gp91^{phox}. The extremely hydrophobic N-terminus of gp91^{phox} is indicated by the checkered bar, and this region is predicted to contain 5~6 transmembrane regions (TMR) which might have two heme groups. The putative FAD binding region (hatched bar) and NADPH binding regions (filled bars) are indicated. A series of truncated forms indicated by the filled bars were constructed as N-terminal fusion proteins with thioredoxin (TRX).

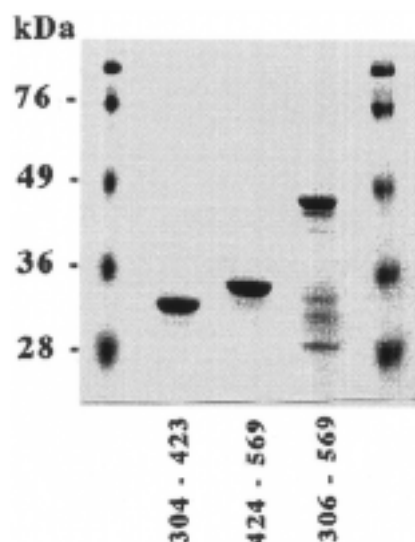


Fig 2. SDS-PAGE of expressed TRX-fusion form of truncated gp91^{phox}. The TRX-His₆-fusion forms of truncated gp91^{phox} were expressed in *E. coli* and were purified by a Ni²⁺-chelating column as described in Materials and Methods. The purified proteins were subjected to SDS-PAGE on a 12% (w/v) polyacrylamide gel, and were visualized by Coomassie-Blue staining. The apparent molecular sizes of TRX fusion forms of gp91^{phox} (304~423), gp91^{phox} (424~569), and gp91^{phox} (306~569) were 32, 34.5, and 48 kDa respectively.

Ni²⁺-chelate affinity matrix. The proteins were purified under denaturing conditions, since TRX-gp91^{phox} (304~423) and TRX-gp91^{phox} (306~569) in particular were poorly soluble and were not retained on a His₆ matrix under non-denaturing conditions, despite the fact that they were highly expressed. In contrast, TRX-gp91^{phox} (424~569) was highly expressed and showed good recovery in the presence or absence of 8 M urea. All purified proteins corresponded in size to their predicted molecular weights on SDS-PAGE (Fig. 2).

Physical properties of expressed proteins:

Although the flavoprotein domain of gp91^{phox} [TRX-gp91^{phox} (304~423), TRX-gp91^{phox} (424~569), and TRX-gp91^{phox} (306~569)] were obtained in soluble form that showed no apparent turbidity, they appeared to be an aggregate of 4 or more monomers. TRX-gp91^{phox} (306~569) preincubated with 0.1 mM FAD was chromatographed on a Sephacryl S-300 column equilibrated with 20 mM Tris-HCl buffer, pH 7.4, containing 50 mM NaCl. The proteins eluted at or near the void volume (MW = 200 kDa). On a SDS-PAGE in the absence of DTT, they migrated as large molecular size (apparent size was greater than 106 kDa) smeared band (data not shown). However, when the proteins were treated with SDS sample buffer containing 80 mM DTT, they gave the correct predicted molecular weights of 32, 34.5, and 48 kDa respectively on a 12% SDS-PAGE gel (Fig. 2). The results imply that the

recombinant gp91^{phox} exists in a polymerized state in ordinary buffer even in the presence of detergent unless reducing agent is added, suggesting that there might be intermolecular disulfide bridges. However, DTT interfered with diaphorase assays (below) and was therefore not included.

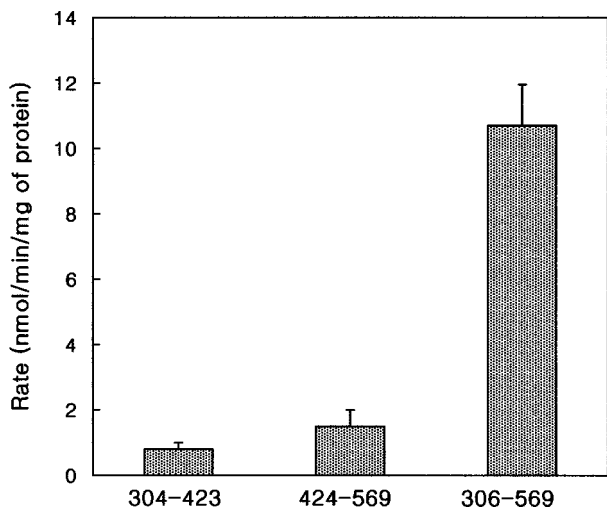


Fig 3. NBT reductase activity of TRX-gp91^{phox}. Each form of TRX-gp91^{phox} was preincubated with an equimolar amount of FAD for 16 hrs at 4°C as described under Materials and Methods. NBT reductase activity was measured using 4 mM of each protein and 200 mM arachidonate in a volume of 50 ml. The reaction was initiated by the addition of 10 ml of this mixture to a 240 ml solution containing 0.2 mM of NBT in the presence of 0.2 mM NADPH. Error bars show the standard error of the mean (n = 3).

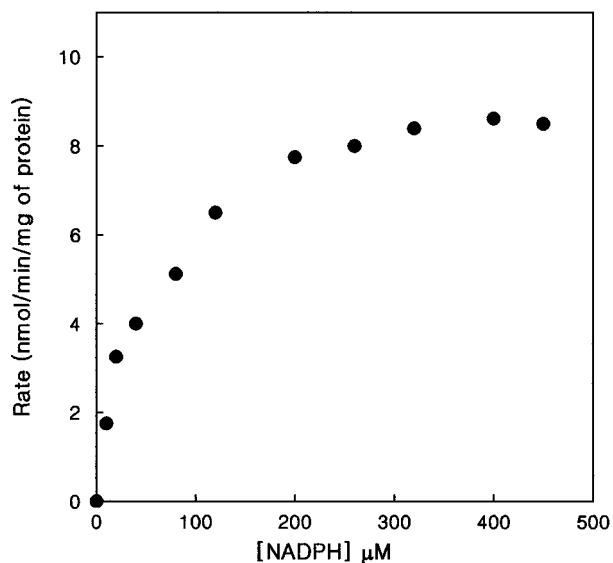


Fig 4. NADPH-dependent NBT reductase activity of TRX-gp91^{phox} (306-569). The assay conditions were as described in Fig 3., except that the reaction was initiated by the addition of 10 ml of the activation mixture to a 240 ml solution containing 0.2 mM of NBT and the indicated concentrations of NADPH.

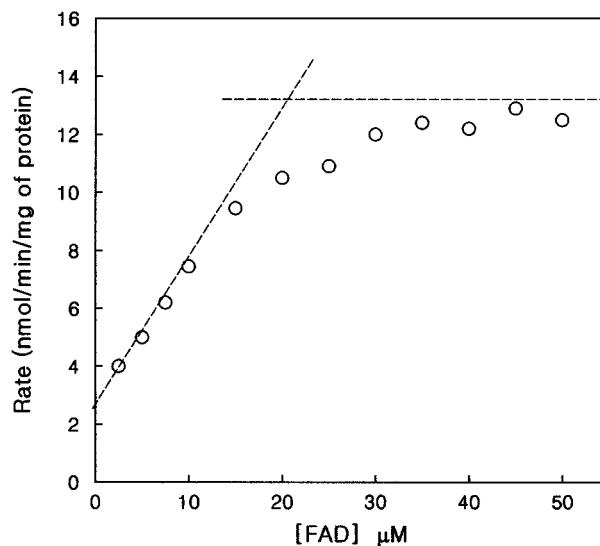


Fig 5. FAD-dependent NBT reductase activity of TRX-gp91^{phox} (306-569). TRX-gp91^{phox} (306-569) (20 mM) was preincubated with varying concentrations of FAD for 16 hrs at 4°C as indicated. NBT reduction of the FAD-reconstituted preparations was measured as described under Materials and Methods using 4 mM TRX-gp91^{phox} (306-569) and 200 mM arachidonate in a 50 ml volume.

NADPH-dependent NBT reductase activities of TRX-gp91^{phox} (306-569):

The longest fusion protein, TRX-gp91^{phox} (306-569), showed NADPH-dependent activity (Fig. 3) whereas the shorter forms, TRX-gp91^{phox} (304-423) and TRX-gp91^{phox} (424-569), showed only background NBT reductase activity (Fig. 3). The K_m for NADPH in the longest protein was determined to be 45 mM (Fig. 4) in the absence of cytosolic factors. This value is similar to the K_m for NADPH (~50 μM) observed in the intact phagocyte NADPH oxidase [15].

FAD-dependent NBT reductase activities of TRX-gp91^{phox} (306-569):

Activity was dependent on FAD (Fig. 5), and increased more or less linearly up to a ratio of FAD/protein of approximately 1 : 1, approaching saturation thereafter. Curve fitting revealed an apparent K_d of 740 nM for binding of a single FAD to the protein. The relatively tight binding of FAD and the normal K_m for NADPH suggest that the flavoprotein domain of TRX-gp91^{phox} (306-569) achieves a more-or-less native structure following expression and renaturation. The observation of a stoichiometry of FAD binding to protein near 1 : 1 suggests that despite its polymeric state, most of the flavoprotein domain is in an active form.

Inhibition of NBT reductase activity of TRX-gp91^{phox} (306-569):

NBT reductase activity of TRX-gp91^{phox} (306-569) was

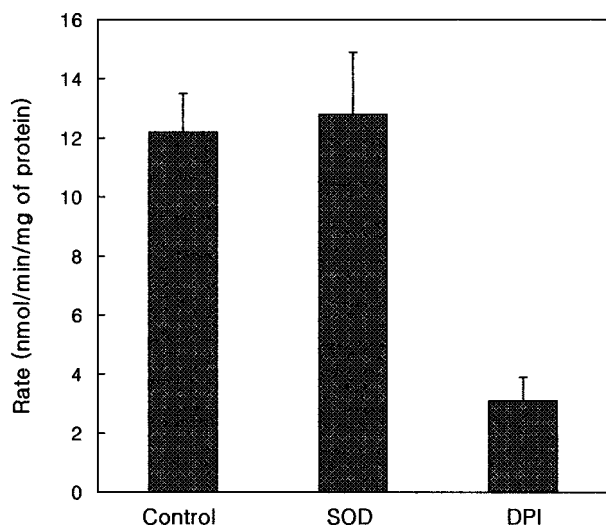


Fig 6. Inhibition of NBT reductase activity of TRX-gp91^{phox} (306~569). NBT reduction was measured using 4 mM of FAD-preloaded TRX-gp91^{phox} (306~569) and 200 mM arachidonate in a 50 ml volume in the presence or absence of either 10 units superoxide dismutase (SOD) or 10 mM diphenylene iodonium (DPI). Error bars show the standard error of the mean (n = 3).

not inhibited by superoxide dismutase (Fig. 6) indicating that NBT reduction was not mediated by superoxide. Thus, it seems likely that NBT accepts electrons directly from the reduced FAD. DPI, a known inhibitor of NADPH-dependent superoxide generation by the intact phagocyte oxidase [9], blocked NADPH-dependent NBT reduction (Fig. 6).

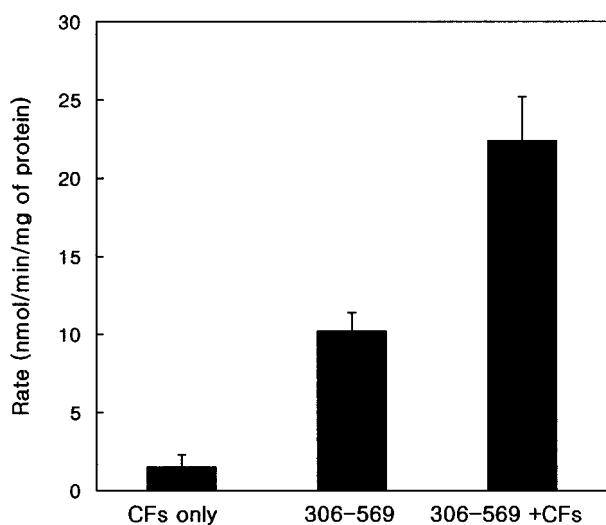


Fig 7. Effects of cytosolic factors (CFs) on NBT reductase activity of TRX-gp91^{phox} (306-569). TRX-gp91^{phox} (306-569) (20 mM) was preincubated with 20 mM of FAD for 16 hrs at 4° C before use. NBT reduction was measured using 4 mM of FAD preloaded TRX-gp91^{phox} (306-569) and 200 mM arachidonate in a volume of 50 ml in the presence or absence of the cytosolic factors (4.8 mM p67^{phox}, 4.2 mM p47^{phox}, 5.4 mM Rac1). Error bars show the standard error of the mean (n=3).

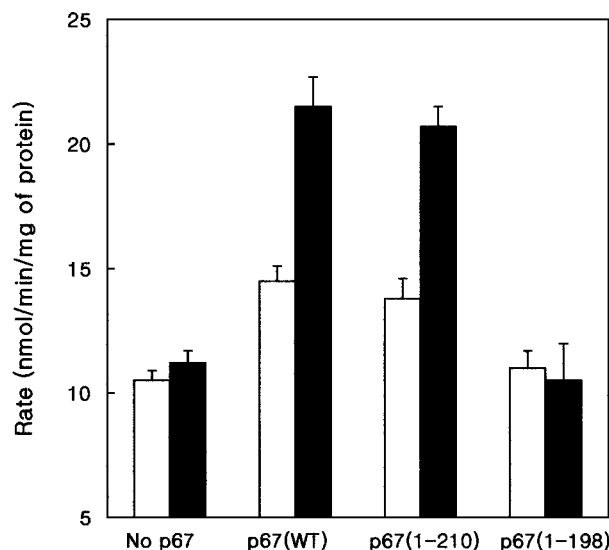


Fig 8. Effects of truncation in the activation domain of p67^{phox} on NBT reductase activity of TRX-gp91^{phox} (306-569). The assay conditions were as in Fig 7, except that in the presence (filled bars) or absence (open bars) of Rac1 (5.4 mM). Error bars show the standard error of the mean (n = 3).

Effects of cytosolic regulatory factors on the NBT reductase activity of TRX-gp91^{phox} (306-569):

As shown in Figure 7, the NBT reductase activity of TRX-gp91^{phox} (306~569) increased nearly 2-fold in the presence of the cytosolic regulatory proteins p47^{phox}, p67^{phox}, and Rac1 (GTPγS). Activity was dependent upon TRX-gp91^{phox} (306~569), and cytosolic factors alone showed almost no activity. Thus, one or more cytosolic regulatory proteins can stimulate NBT reductase activity of TRX-gp91^{phox} (306~569). To further explore the requirement for cytosolic factors, the activity was measured in the presence of combinations of cytosolic factors. Elimination of p47^{phox} had no effect on NBT reductase activity (not shown). As shown in Fig. 8, p67^{phox} stimulated the activity in the absence of other cytosolic factors. Rac alone had little or no stimulatory effect, but increased the magnitude of stimulation by p67^{phox} (Fig. 8). The effect of the activation domain of p67^{phox} on NBT reductase activity of the flavoprotein domain was also investigated. p67^{phox} (1-210) which contains the activation domain stimulated activity as well as the wild type p67^{phox}. However, p67^{phox} (1-198) which lacks the activation domain was ineffective (Fig. 8).

Discussion

Based on previous models, the globular portion of the b subunit of cytochrome b₅₅₈ is largely exposed to the solvent, and accessible to NADPH from the cytoplasm [48]. Several flavin-dependent reductases possess a b-stranded barrel structure for FAD binding [30]. The sequence alignment of FAD binding domain of gp91^{phox}

and ferredoxin-NADP⁺ reductase family showed that the amino acid residues 279-400 of gp91^{phox} is homologous to a general FAD binding structure [53]. The HPFT motif (residues 338-341) in this structure is predicted to interact directly with FAD in the flavocytochrome b₅₅₈ model [48], and is conserved in gp91^{phox} in human, porcine, and mouse [55, 3]. The aim of this study was to express a flavo-protein-homology domain of cytochrome b₅₅₈ which lacks the transmembrane heme-binding regions, and to investigate its catalytic properties. gp91^{phox} (306-569) includes most of the predicted b-stranded barrel structure including the HPFT motif and also contains regions which are predicted to form the NADPH binding site (Fig.1). This structure was successfully expressed as a TRX fusion protein and showed low catalytic activity (NBT reductase activities). However, the maximal rate of NBT reduction at saturating FAD concentration was low, about 4 electrons/min/molecule of protein. The low activity may either be an intrinsic property of the flavoprotein domain, or may indicate that the expressed flavoprotein is catalytically inefficient due to its cross-linked nature or absence of an appropriate conformation. In a previous study, the anaerobic rate of FAD reduction was less than 1% of the aerobic rate [25], and the authors proposed that oxygen induces a conformation which favors flavin reduction. Since there is no heme in TRX-gp91^{phox} (306-569), such a conformational regulation may not be possible. The intact flavocytochrome also catalyzes a low rate of INT reduction [10], but this rate is still approximately 100-200 fold higher than that seen in the present study, suggesting either a less efficient electron transfer in the expressed flavoprotein domain, or additional electron transfer mechanisms in the intact cytochrome. The low activity may make this preparation of limited utility for mechanistic studies, but the model system appears to be adequate for drawing a number of important conclusions.

The diaphorase activity of TRX-gp91^{phox} (306-569) was dependent upon FAD which showed a relatively high binding affinity ($K_d = 740$ nM). The expressed domain also showed a K_m for NADPH of around 50 μ M, the same value which is seen for the NADPH-superoxide generating activity of the intact respiratory burst oxidase. These data indicate that the expressed, renatured protein forms a reasonably intact structure, sufficient to bind both NADPH and FAD and to catalyze a diaphorase activity, albeit at a very low rate. These data demonstrate unequivocally that this domain contains binding sites for both an NADPH and an FAD. Although it is possible that p67^{phox} also contains a binding site for NADPH, as was recently proposed [46], these data do not support the idea that such a site is involved in catalysis.

Importantly, these studies also reveal that the flavo-protein domain is the target of regulation by p67^{phox}. Previously, we showed that an activation domain in p67^{phox}

(residues 199-210) is essential for NADPH-oxidase activation in a cell-free system [18]. Truncated forms of p67^{phox} lacking this region showed no ability to activate the oxidase, despite that fact that these forms bound normally to oxidase components and assembled normally as part of the oxidase complex under cell-free activation conditions. As shown in Fig. 8, the truncation of the activation domain eliminated the ability of p67^{phox} to activate the NBT-reductase activity of the flavoprotein domain. These data indicate that the target of the activation domain of p67^{phox} resides within the flavoprotein domain of gp91^{phox}. These data provide a physical explanation for data indicating that the activation domain of p67^{phox} controls the reduction of FAD by NADPH [32]. Interestingly, this study showed that p67^{phox} had little or no effect on NADPH binding, but data were most consistent with regulation of electron/hydride transfer from NADPH to FAD.

These studies failed to provide evidence for an effect of p47^{phox} on regulation at the level of the flavoprotein domain. We have previously shown that p47^{phox} is not essential for NADPH-dependent superoxide generation by the intact respiratory burst oxidase under cell-free conditions [16]. Its role was proposed to be a regulated adapter protein, since its effect was to enhance the affinity of p67^{phox} and Rac by up to 100-fold. Although Rac does not directly activate the flavoprotein domain, a role for Rac is implied by the present studies, since Rac enhances the effect of p67^{phox}. Direct binding of Rac to p67^{phox} via the effector region on Rac (residues 26-45) has been demonstrated [33], and Rac is known to bind to the plasma membrane through its C-terminus [26]. A third region on Rac, the insert region (residues 124-135) is essential for optimal activity and is involved in protein-protein interactions within the assembled oxidase [33], this region has been proposed to bind to the cytochrome, although this has not yet been directly demonstrated. Rac may be synergizing with p67^{phox} in activating diaphorase activity of the flavoprotein domain either by binding to p67^{phox}, producing an active conformation, or by binding simultaneously to both p67^{phox} and the flavoprotein domain of gp91^{phox}. The present studies do not distinguish between these possibilities, but indicate that Rac somehow synergizes with p67^{phox} to activate the flavoprotein domain of gp91^{phox}. The ability of p67^{phox} to activate NBT reductase activity in the absence of Rac, however, indicates that p67^{phox} must be interacting directly with the flavoprotein domain, and that it is likely to be the primary regulatory element in this complex and elegant system.

References

1. **Badwey JA, Karnovsky ML.** Active oxygen species and the functions of phagocytic leukocytes. *Annu Rev Biochem*, 1980, **49**, 695-726.

2. **Biberstine-Kinkade KJ, Yu L, Dinauer MC.** Mutagenesis of an arginine- and lysine-rich domain in the gp91(*phox*) subunit of the phagocyte NADPH-oxidase flavocytochrome b₅₅₈. *J Biol Chem*, 1999, **274**(15), 10451-7.
3. **Bjorgvinsdottir H, Zhen L, Dinauer MC.** Cloning of murine gp91*phox* cDNA and functional expression in a human X-linked chronic granulomatous disease cell line. *Blood*, 1996, **87**(5), 2005-10.
4. **Bradford MM.** A rapid and sensitive method for the quantitation of microgram quantities of protein utilizing the principle of protein-dye binding. *Anal Biochem*, 1976, **72**, 248-54.
5. **Chanock SJ, el Benna J, Smith RM, Babior BM.** The respiratory burst oxidase. *J Biol Chem*, 1994, **269**(40), 24519-22.
6. **Clark RA, Volpp BD, Leidal KG, Nauseef WM.** Two cytosolic components of the human neutrophil respiratory burst oxidase translocate to the plasma membrane during cell activation. *J Clin Invest*, 1990, **85**(3), 714-21.
7. **Clark RA.** The human neutrophil respiratory burst oxidase. *J Infect Dis*, 1990, **161**(6), 1140-7.
8. **Cross AR, Curnutte JT.** The cytosolic activating factors p47*phox* and p67*phox* have distinct roles in the regulation of electron flow in NADPH oxidase. *J Biol Chem*, 1995, **270**(12), 6543-8.
9. **Cross AR, Jones OT.** The effect of the inhibitor diphenylene iodonium on the superoxide-generating system of neutrophils. Specific labelling of a component polypeptide of the oxidase. *Biochem J*, 1986, **237**(1), 111-6.
10. **Cross AR, Yarchover JL, Curnutte JT.** The superoxide-generating system of human neutrophils possesses a novel diaphorase activity. Evidence for distinct regulation of electron flow within NADPH oxidase by p67-*phox* and p47-*phox*. *J Biol Chem*, 1994, **269**(34), 21448-54.
11. **Dinauer MC, Orkin SH, Brown R, Jesaitis AJ, Parkos CA.** The glycoprotein encoded by the X-linked chronic granulomatous disease locus is a component of the neutrophil cytochrome b complex. *Nature*, 1987, **327**(6124), 717-20.
12. **Dinauer MC, Pierce EA, Bruns GA, Curnutte JT, Orkin SH.** Human neutrophil cytochrome b light chain (p22-*phox*). Gene structure, chromosomal location, and mutations in cytochrome-negative autosomal recessive chronic granulomatous disease. *J Clin Invest*, 1990, **86**(5), 1729-37.
13. **Dorseuil O, Quinn MT, Bokoch GM.** Dissociation of Rac translocation from p47*phox*/p67*phox* movements in human neutrophils by tyrosine kinase inhibitors. *J Leukoc Biol*, 1995, **58**(1), 108-13.
14. **Doussiere J, Brandolin G, Derrien V, Vignais PV.** Critical assessment of the presence of an NADPH binding site on neutrophil cytochrome b₅₅₈ by photoaffinity and immunochemical labeling. *Biochemistry*, 1993, **32**(34), 8880-7.
15. **Doussiere J, Buzenet G, Vignais PV.** Photoaffinity labeling and photoinactivation of the O₂(-)-generating oxidase of neutrophils by an azido derivative of FAD. *Biochemistry*, 1995, **34**(5), 1760-70.
16. **Freeman JL, Lambeth JD.** NADPH oxidase activity is independent of p47*phox* in vitro. *J Biol Chem*, 1996, **271**(37), 22578-82.
17. **Gentz R, Chen CH, Rosen CA.** Bioassay for trans-activation using purified human immunodeficiency virus tat-encoded protein: trans-activation requires mRNA synthesis. *Proc Natl Acad Sci U S A*, 1989, **86**(3), 821-4.
18. **Han CH, Freeman JL, Lee T, Motalebi SA, Lambeth JD.** Regulation of the neutrophil respiratory burst oxidase. Identification of an activation domain in p67(*phox*). *J Biol Chem*, 1998, **273**(27), 16663-8.
19. **Heyworth PG, Bohl BP, Bokoch GM, Curnutte JT.** Rac translocates independently of the neutrophil NADPH oxidase components p47*phox* and p67*phox*. Evidence for its interaction with flavocytochrome b₅₅₈. *J Biol Chem*, 1994, **269**(49), 30749-52.
20. **Heyworth PG, Curnutte JT, Nauseef WM, Volpp BD, Pearson DW, Rosen H, Clark RA.** Neutrophil nicotinamide adenine dinucleotide phosphate oxidase assembly. Translocation of p47-*phox* and p67-*phox* requires interaction between p47-*phox* and cytochrome b₅₅₈. *J Clin Invest*, 1991, **87**(1), 352-6.
21. **Imajoh-Ohmi S, Tokita K, Ochiai H, Nakamura M, Kanegasaki S.** Topology of cytochrome b₅₅₈ in neutrophil membrane analyzed by anti-peptide antibodies and proteolysis. *J Biol Chem*, 1992, **267**(1), 180-4.
22. **Kleinberg ME, Malech HL, Mital DA, Leto TL.** p21rac does not participate in the early interaction between p47-*phox* and cytochrome b558 that leads to phagocyte NADPH oxidase activation in vitro. *Biochemistry*, 1994, **33**(9), 2490-5.
23. **Koshkin V, Lotan O, Pick E.** Electron transfer in the superoxide-generating NADPH oxidase complex reconstituted in vitro. *Biochim Biophys Acta*, 1997, **1319**(2-3), 139-46.
24. **Koshkin V, Lotan O, Pick E.** The cytosolic component p47(*phox*) is not a sine qua non participant in the activation of NADPH oxidase but is required for optimal superoxide production. *J Biol Chem*, 1996, **271**(48), 30326-9.
25. **Koshkin V, Pick E.** Superoxide production by cytochrome b559. Mechanism of cytosol-independent activation. *FEBS Lett*, 1994, **338**(3), 285-9.
26. **Kreck ML, Uhlinger DJ, Tyagi SR, Inge KL, Lambeth JD.** Participation of the small molecular weight GTP-binding protein Rac1 in cell-free activation and assembly of the respiratory burst oxidase. Inhibition by a carboxyl-terminal Rac peptide. *J Biol Chem*, 1994, **269**(6), 4161-8.
27. **LaVallie ER, DiBlasio EA, Kovacic S, Grant KL, Schendel PF, McCoy JM.** A thioredoxin gene fusion expression system that circumvents inclusion body formation in the *E. coli* cytoplasm. *Biotechnology (N Y)*, 1993, **11**(2), 187-93.
28. **Mitchell JA, Kohlhaas KL, Matsumoto T, Pollock JS, Forstermann U, Warner TD, Schmidt HH, Murad F.** Induction of NADPH-dependent diaphorase and nitric oxide synthase activity in aortic smooth muscle and cultured macrophages. *Mol Pharmacol*, 1992, **41**(6), 1163-8.
29. **Nakamura M, Sendo S, van Zwieten R, Koga T, Roos D, Kanegasaki S.** Immunocytochemical discovery of the 22- to 23-Kd subunit of cytochrome b₅₅₈ at the surface of human

- peripheral phagocytes. *Blood*, 1988, **72**(5), 1550-2..
30. **Nishida H, Inaka K, Miki K.** Specific arrangement of three amino acid residues for flavin-binding barrel structures in NADH-cytochrome b5 reductase and the other flavin-dependent reductases. *FEBS Lett*, 1995, **361**(1), 97-100.
 31. **Nisimoto Y, Freeman JLR, Motalebi SA, Hirshberg M, Lambeth JD.** Rac binding to p67(phox). Structural basis for interactions of the Rac1 effector region and insert region with components of the respiratory burst oxidase. *J Biol Chem*, 1997, **272**(30), 18834-41.
 32. **Nisimoto Y, Motalebi S, Han CH, Lambeth JD.** The p67(phox) activation domain regulates electron flow from NADPH to flavin in flavocytochrome b(558). *J Biol Chem*, 1999, **274**(33), 22999-3005.
 33. **Nisimoto Y, Otsuka-Murakami H, Lambeth DJ.** Reconstitution of flavin-depleted neutrophil flavocytochrome b558 with 8-mercapto-FAD and characterization of the flavin-reconstituted enzyme. *J Biol Chem*, 1995, **270**(27), 16428-34.
 34. **Nomanbhoy TK, Cerione R.** Characterization of the interaction between RhoGDI and Cdc42Hs using fluorescence spectroscopy. *J Biol Chem*, 1996, **271**(17), 10004-9.
 35. **Parkos CA, Dinauer MC, Walker LE, Allen RA, Jesaitis AJ, Orkin SH.** Primary structure and unique expression of the 22-kilodalton light chain of human neutrophil cytochrome b. *Proc Natl Acad Sci USA*, 1988, **85**(10), 3319-23.
 36. **Quinn MT, Evans T, Loetterle LR, Jesaitis AJ, Bokoch GM.** Translocation of Rac correlates with NADPH oxidase activation. Evidence for equimolar translocation of oxidase components. *J Biol Chem*, 1993, **268**(28), 20983-7.
 37. **Ragan CI, Bloxham DP.** Specific labelling of a constituent polypeptide of bovine heart mitochondrial reduced nicotinamide-adenine dinucleotide-ubiquinone reductase by the inhibitor diphenylethylidonium. *Biochem J*, 1977, **163**(3), 605-15.
 38. **Ravel P, Lederer F.** Affinity-labeling of an NADPH-binding site on the heavy subunit of flavocytochrome b558 in particulate NADPH oxidase from activated human neutrophils. *Biochem Biophys Res Commun*, 1993, **196**(2), 543-52.
 39. **Rotrosen D, Kleinberg ME, Nunoi H, Leto T, Gallin JJ, Malech HL.** Evidence for a functional cytoplasmic domain of phagocyte oxidase cytochrome b558. *J Biol Chem*, 1990, **265**(15), 8745-50.
 40. **Rotrosen D, Yeung CL, Leto TL, Malech HL, Kwong CH.** Cytochrome b558: the flavin-binding component of the phagocyte NADPH oxidase. *Science*, 1992, **256**(5062), 1459-62.
 41. **Royer-Pokora B, Kunkel LM, Monaco AP, Goff SC, Newburger PE, Baehner RL, Cole FS, Curnutte JT, Orkin SH.** Cloning the gene for an inherited human disorder-chronic granulomatous disease--on the basis of its chromosomal location. *Nature*, 1986, **322**(6074), 32-8.
 42. **Sambrook, J., Fritsch, E. F., and Maniatis, T. Molecular Cloning: A Laboratory Manual 2nd Ed.,** Cold Spring Harbor Laboratory, Cold Spring Harbor, NY, 1989.
 43. **Segal AW, Abo A.** The biochemical basis of the NADPH oxidase of phagocytes. *Trends Biochem Sci*, 1993, **18**(2), 43-7.
 44. **Segal AW, West I, Wientjes F, Nugent JH, Chavan AJ, Haley B, Garcia RC, Rosen H, Scrace G.** Cytochrome b-245 is a flavocytochrome containing FAD and the NADPH-binding site of the microbicidal oxidase of phagocytes. *Biochem J*, 1992, **284** (Pt 3), 781-8.
 45. **Segal AW.** Absence of both cytochrome b-245 subunits from neutrophils in X-linked chronic granulomatous disease. *Nature*, 1987, **326**(6108), 88-91.
 46. **Smith RM, Connor JA, Chen LM, Babior BM.** The cytosolic subunit p67 phox contains an NADPH. *J Clin Invest*, 1996, **98**(4), 977-83.
 47. **Sumimoto H, Sakamoto N, Nozaki M, Sakaki Y, Takeshige K, Minakami S.** Cytochrome b₅₅₈, a component of the phagocyte NADPH oxidase, is a flavoprotein. *Biochem Biophys Res Commun*, 1992, **186**(3), 1368-75.
 48. **Taylor WR, Jones DT, Segal AW.** A structural model for the nucleotide binding domains of the flavocytochrome b-245 beta-chain. *Protein Sci*, 1993, **2**(10), 1675-85.
 49. **Teahan C, Rowe P, Parker P, Totty N, Segal AW.** The X-linked chronic granulomatous disease gene codes for the beta-chain of cytochrome b-245. *Nature*, 1987, **327**(6124), 720-1.
 50. **Tyagi SR, Neckelmann N, Uhlinger DJ, Burnham DN, Lambeth JD.** Cell-free translocation of recombinant p47-phox, a component of the neutrophil NADPH oxidase. *Biochemistry*, 1992, **31**(10), 2765-74.
 51. **Uhlinger DJ, Taylor KL, Lambeth JD.** p67-phox enhances the binding of p47-phox to the human neutrophil respiratory burst oxidase complex. *J Biol Chem*, 1994, **269**(35), 22095-8.
 52. **Uhlinger DJ, Tyagi SR, Inge KL, Lambeth JD.** The respiratory burst oxidase of human neutrophils. Guanine nucleotides and arachidonate regulate the assembly of a multicomponent complex in a semirecombinant cell-free system. *J Biol Chem*, 1993, **268**(12), 8624-31.
 53. **Yoshida LS, Saruta F, Yoshikawa K, Tatsuzawa O, Tsunawaki S.** Mutation at histidine 338 of gp91(phox) depletes FAD and affects expression of cytochrome b558 of the human NADPH oxidase. *J Biol Chem*, 1998, **273**(43), 27879-86.
 54. **Yu L, Quinn MT, Cross AR, Dinauer MC.** Gp91(phox) is the heme binding subunit of the superoxide-generating NADPH oxidase. *Proc Natl Acad Sci USA*, 1998, **95**(14), 7993-8.
 55. **Zhou Y, Lin G, Murtaugh MP.** Interleukin-4 suppresses the expression of macrophage NADPH oxidase heavy chain subunit (gp91-phox). *Biochim Biophys Acta*, 1995, **1265**(1), 40-8.